Sanes, J. R., Schachner, M., & Covault, J. (1986) *J. Cell Biol. 102*, 420.
Schauer, R. (1978) *Methods Enzymol. 50*, 64.
Sell, S., & Ruoslahti, E. (1982) *JNCI J. Natl. Cancer Inst. 69*, 1105.
Shibata, S., Peters, B. P., Roberts, D. D., Goldstein, I. J., & Liotta, L. A. (1982) *FEBS Lett. 142*, 194.
Shibuya, N., Goldstein, I. J., Broekaert, W. F., Nsimba-Lubaki, M., Peeters, B., & Peumans, W. J. (1987) *Arch. Biochem. Biophys. 254*, 1.
Spiro, R. G., & Bhoyroo, V. D. (1984) *J. Biol. Chem. 259*, 9858.
Stellner, K., Saitz, H., & Hakomori, S. (1973) *Arch. Biochem. Biophys. 155*, 464.
Takasaki, S., Murray, G. J., Furbish, F. S., Brady, R. O., Barranger, J. A., & Kobata, A. (1984) *J. Biol. Chem. 259*, 10112.
Terranova, V. P., Liotta, L. A., Russo, R. G., & Martin, G. R. (1980) *Cell 22*, 719.
Terranova, V. P., Rao, C. N., Kalebic, T., Margulies, I. M., & Liotta, L. A. (1983) *Proc. Natl. Acad. Sci. U.S.A. 80*, 444.
Terranova, V. P., Williams, J. E., Liotta, L. A., & Martin, G. R. (1984) *Science 226*, 982.
Timpl, R., Rohde, H., Robey, P. G., Rennard, S. I., Foidart, J. M., & Martin, G. M. (1979) *J. Biol. Chem. 254*, 9933.
Timpl, R., Dziadek, M., Fujiwara, S., Nowack, H., & Wick, G. (1983) *Eur. J. Biochem. 137*, 455.
Varani, J., Grimstad, I. A., Knibbs, R. N., Hovig, T., & McCoy, J. P. (1985) *Clin. Exp. Metastasis 3*, 45.
Wang, W. C., & Cummings, R. D. (1988) *J. Biol. Chem. 263*, 4576.
Warren, L. (1959) *J. Biol. Chem. 234*, 1971.
Wicha, M. S., & Huard, T. K. (1983) *Exp. Cell Res. 143*, 475.
Yamamoto, K., Tsuji, T., Tarutani, O., & Osawa, T. (1984) *Eur. J. Biochem. 143*, 133.
Yamashita, K., Tachibana, Y., Nakayama, T., Kitamura, M., Endo, Y., & Kobata, A. (1980) *J. Biol. Chem. 255*, 5635.
Yamashita, K., Mizuochi, T., & Kobata, A. (1982) *Methods Enzymol. 83*, 105.
Zhu, B. R. C., & Laine, R. A. (1985) *J. Biol. Chem. 260*, 4041.

Environmental Modulation of M13 Coat Protein Tryptophan Fluorescence Dynamics†

Iain D. Johnson and Bruce S. Hudson*
Department of Chemistry and Molecular Biology Institute, University of Oregon, Eugene, Oregon 97403
Received October 13, 1988; Revised Manuscript Received March 7, 1989

ABSTRACT: The effects of detergent [deoxycholate (DOC)] and phospholipid [dimyristoylphosphatidylcholine (DMPC)] environments on the rotational dynamics of the single tryptophan residue 26 of bacteriophage M13 coat protein have been investigated by using time-resolved single photon counting measurements of the fluorescence intensity and anisotropy decay. The total fluorescence decay of tryptophan-26 is complex but rather similar in DOC as compared to DMPC when analyzed in terms of a lifetime distribution (exponential series method). This similarity, in conjunction with the almost identical steady-state fluorescence spectra, indicates only minor differences between the tryptophan environments in DOC and DMPC. The reorientational dynamics of tryptophan-26 are dominated by slow rotation of the entire protein in both detergent and phospholipid environments. The resolved anisotropy decay in DOC can be approximated by a simple hydrodynamic model of protein/detergent micelle rotational diffusion, although the data indicate slightly greater complexity in the rotational motion. The tryptophan fluorescence anisotropy is not sensitive to protein conformational changes in DOC detected by nuclear magnetic resonance on the basis of pH independence in the range 7.5–9.1. In DMPC bilayers, restricted tryptophan motion with a correlation time of approximately 2 ns is observed together with a second very slow reorientational component. Resolution of the time constant for this slow rotation is obscured by the tryptophan fluorescence time window being too short to clearly locate its anisotropic limit. The possible contribution made by axial rotational diffusion of the protein to this slow rotational process is discussed. The fluorescence intensity and anisotropy decays are sensitive to the DMPC thermal phase transition, indicating that tryptophan-26 is in direct contact with phospholipid acyl chains.

The major coat protein of bacteriophage M13 (M13-CP)[1] and the homologous fd and fl coat proteins are comprised of 50 amino acid residues (M_r 5240) in a sequence that has a predominantly acidic N-terminal region, a basic C-terminal region, and a highly hydrophobic core (Asbeck et al., 1969; Nakashima & Konigsberg, 1974). The core region (residues 21–39) contains a single tryptophan residue at position 26. The protein is of interest in terms of bacteriophage assembly

† Supported by NIH Grant GM26536. A preliminary account of this work was presented at the 1986 Biophysical Society Annual Meeting, San Francisco, CA (Johnson et al., 1986).
* Address correspondence to this author at the Department of Chemistry, University of Oregon.

[1] Abbreviations: M13-CP, bacteriophage M13 gene 8 (coat) protein; DOC, sodium deoxycholate; DMPC, dimyristoylphosphatidylcholine; NMR, nuclear magnetic resonance; CD, circular dichroism; 16-DS, 16-doxylstearic acid.

0006-2960/89/0428-6392$01.50/0

mechanisms (Nozaki et al., 1976) and as a general model for protein insertion in membranes (Wickner, 1988). In both areas, the ability of the protein to adopt multiple conformational states is believed to be functionally significant.

Several spectroscopic studies have demonstrated the existence of multiple M13-CP conformations in both phospholipid bilayers and detergent micelles (Nozaki et al., 1978; Fodor et al., 1981; Dunker et al., 1982; Wilson & Dahlquist, 1985). Interconversion of these conformations appears to involve substantial structural rearrangement and be dependent on the chemical nature of the surrounding environment (Fodor et al., 1981; Wilson & Dahlquist, 1985). At the supramolecular level, the protein exists in a minimum dimeric aggregation state in both phospholipids and detergents (Makino et al., 1975; Nozaki et al., 1978; Bayer & Feigenson, 1985). The orientation of the protein when reconstituted in phospholipid bilayer membranes remains subject to some uncertainty, despite recent improvements in analysis methods (Bayer & Feigenson, 1985).

The dynamics of M13-CP have been extensively studied by NMR techniques. In both phospholipids (Leo et al., 1987) and detergents (Henry et al., 1986, 1987), the polypeptide backbone is found to be rigid in the central segment but mobile in both terminal regions. Analysis of side chain motions indicates that tryptophan-26 is immobile in sodium dodecyl sulfate micelles (Cross & Opella, 1981) and DMPC bilayers (Leo et al., 1987).

Previous work in this laboratory has utilized M13-CP incorporated in DMPC vesicles by the cholate dilution method (Wickner, 1976, 1977) as a model system in which to examine protein effects on lipid structure and dynamics as monitored by parinaric acid fluorescence (Kimelman et al., 1979; Wolber & Hudson, 1982). Here, we present experiments with the converse perspective—that of protein dynamics monitored by time-resolved intrinsic tryptophan fluorescence (Beechem & Brand, 1985). It is shown that tryptophan-26 of M13-CP in DMPC bilayers has restricted reorientational mobility with a temperature-dependent amplitude and a relaxation time of 1–3 ns that depends on lipid chain mobility. Slower reorientational motion is also detected due to overall particle rotation in DOC micelles and axial protein rotation in DMPC bilayers. The fluorescence intensity decay of M13-CP tryptophan-26 is complex in both DOC micelles and DMPC bilayers. The similarity of the fluorescence decay behavior in these two hydrophobic environments becomes apparent when the data are interpreted in terms of lifetime distributions.

Materials and Methods

Materials. M13-CP was purified from disrupted bacteriophage by column chromatography as described by Wilson and Dahlquist (1985). Protein concentrations were assayed spectrophotometrically by using $\epsilon_{280nm} = 1.65$ cm^2 mg^{-1} (Nozaki et al., 1976). DMPC was purchased from Sigma (St. Louis, MO) and was purified on a 1.5-m column of Sephadex LH20 eluted with absolute ethanol. Cholic acid and deoxycholic acid were obtained from Sigma (St. Louis, MO) and were recrystallized twice from ethanol and converted to aqueous solutions of sodium salts by addition of concentrated NaOH. Dialysis tubing (Spectrapor 3, molecular weight cutoff 3500) was obtained from VWR Scientific Inc. 16-Doxylstearic acid (16-DS) from Sigma (St. Louis, MO) was dissolved in spectroscopic-grade methanol.

Sample Preparation. M13-CP solutions were prepared by dialysis of DOC-solubilized fractionated protein (2 mL) in 20 mM $NaHCO_3$/30 mM DOC, pH 8.5, (500 mL) at 4 °C for 24 h. Samples were diluted to about 30 μM protein for fluorescence experiments. Where necessary, pH adjustments were made by addition of 1.0 M NaOH or HCl monitored by an Orion Research Model 501 pH meter. M13-CP was incorporated into DMPC vesicles at a lipid to protein ratio of 70:1 mol/mol by the cholate dilution method (Wickner, 1976, 1977; Kimelman et al., 1979). A clear solution containing 1.8 mg of protein and 16 mg of DMPC in 1.4 mL of 1% (w/v) sodium cholate was incubated at 23 °C for 30 min and then diluted into 50 mL of 0.05 M potassium phosphate buffer, pH 7.0, at the same temperature. Turbidity indicative of vesicle formation was observed within 10 min of dilution. After 1-h incubation, vesicles were collected by centrifugation at 45000g for 1 h and washed with 50 mL of suspension buffer. This procedure results in vesicles with a diameter of approximately 200 nm in which the M13-CP spans the lipid bilayer (Wickner, 1977).

Fluorescence Instrumentation. Corrected fluorescence emission spectra were recorded on an SLM-8000 spectrofluorometer (SLM Industries, Urbana, IL). Time-resolved single photon counting techniques (O'Connor & Phillips, 1984) were used for total fluorescence and anisotropy decay measurements. The instrumentation and data collection procedures have been described in detail elsewhere (Ruggiero & Hudson, 1989). The principal components were a cavity-dumped rhodamine 6G dye laser synchronously pumped by the second harmonic output of a Spectra-Physics 3460 mode-locked Nd:YAG laser for excitation and a Hamamatsu R1294U electrostatically focused microchannel plate photomultiplier for detection. The instrument response function was typically 200 ps wide at half-maximum. Fluorescence excitation for all measurements was at 300 nm with detection at 340 nm through a 10-nm band-pass Corion interference filter. The data collection limit was typically 60 000 counts peak channel (7×10^6 counts integral) for total fluorescence decays (54.7° polarization with vertical excitation). For anisotropy decays, the peak channel difference between the vertically and horizontally polarized components was 30 000 counts (3×10^6 counts integral). The time base was 40 ps/channel in a total of 1024 channels.

Data Analysis. Time-resolved fluorescence data were analyzed by nonlinear least-squares iterative reconvolution (Grinvald & Steinberg, 1974) using the following fit quality criteria: reduced χ^2, weighted residuals, residual autocorrelation, and runs test (Gunst & Mason, 1980). The vertical and horizontal polarized components of the anisotropy data were analyzed by simultaneous optimization of total fluorescence and anisotropy decay parameters (Cross & Fleming, 1984). Both total fluorescence [$I(t)$] and anisotropy [$r(t)$] decays were represented by sums of exponentials:

$$I(t) = \sum_i \alpha_i \exp(-t/\tau_i)$$

$$r(t) = \sum_j r_j \exp(-t/\phi_j)$$

No exclusive associations of $I(t)$ and $r(t)$ components were assumed (Ludescher et al., 1987; Hudson et al., 1987). Anisotropy decay analyses were truncated at short time (commencing at the total fluorescence intensity maximum) to avoid distortions in the rising edge data due to excitation light scattered by the faintly turbid vesicle samples. This procedure entails some loss of short time resolution (Cross & Fleming, 1984). For total fluorescence decays, the entire data range was analyzed by inclusion of an additional amplitude term in the fitting function to correct for scattered excitation. Total fluorescence decays were also analyzed by the exponential series method described by James and Ware (1986) in which the amplitudes of a series of equally spaced fixed lifetimes are varied to optimally fit the data. Lifetimes with amplitudes

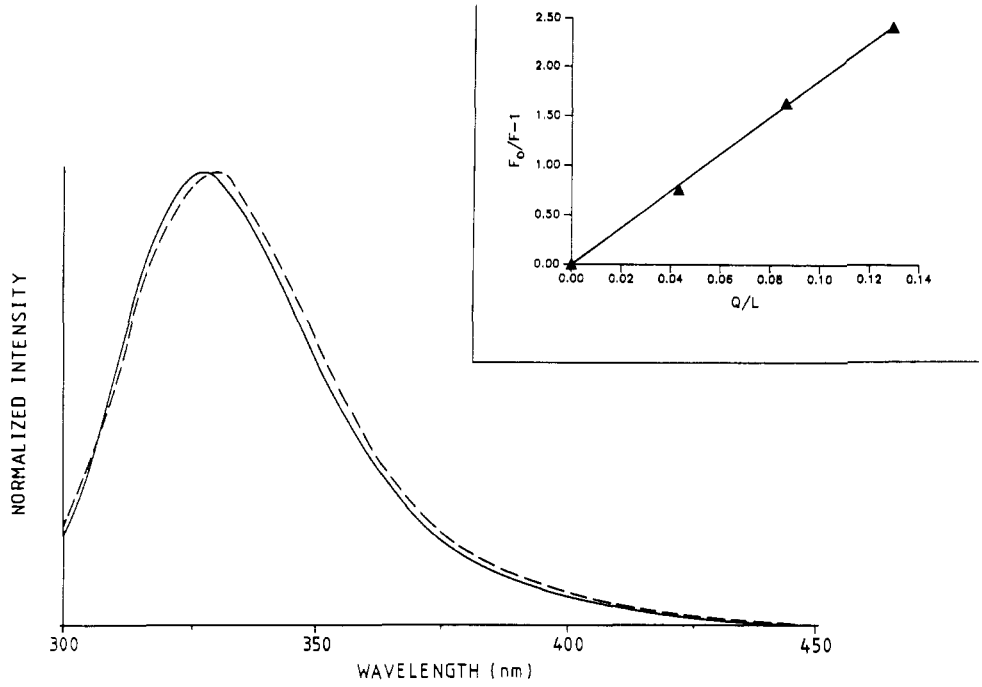

FIGURE 1: Corrected fluorescence emission spectra (2-nm band-pass) of M13-CP tryptophan-26 in DOC (—) and DMPC (---) at 20 °C. Excitation at 295 nm (4-nm band-pass). Inset: Quenching of tryptophan fluorescence in DMPC bilayers at 30 °C by 16-DS added from a 0.02 M stock solution in methanol. Q/L represents the molar ratio of quencher to lipid. F_0 represents the initial unquenched fluorescence intensity, and F is the quenched fluorescence intensity, both measured at 335 nm with 295-nm excitation.

Table I: Parameters Representing Fits of i Exponentials (i = 3, 4) to Total Fluorescence Decays of M13-CP Tryptophan-26 in DOC and DMPC at 20 °C

	i	α_1	τ_1 (ns)	α_2	τ_2 (ns)	α_3	τ_3 (ns)	α_4	τ_4 (ns)	$\langle\tau\rangle$ (ns)	χ^2
DOC	3	0.22	0.81	0.41	3.36	0.37	6.38			5.06	1.141
DMPC	3	0.24	0.68	0.53	3.48	0.24	6.98			4.94	1.507
±		0.01	0.02	0.01	0.05	0.01	0.05				
DOC	4	0.14	0.20	0.29	1.41	0.45	4.35	0.19	7.09	5.06	0.976
DMPC	4	0.21	0.16	0.22	1.42	0.48	4.36	0.09	8.27	4.96	1.083
±		0.01	0.02	0.01	0.06	0.02	0.12	0.02	0.24		

[a] $\langle\tau\rangle = \sum_i \alpha_i \tau_i^2 / \sum_i \alpha_i \tau_i$.

which fall below a set threshold (0.5% of maximum) are eliminated from the analysis.

Results

Comparison of Tryptophan Fluorescence in DOC and DMPC. Corrected fluorescence emission spectra of M13-CP tryptophan-26 in DOC and DMPC shown in Figure 1 are almost identical. The maxima at 330 nm in DMPC [also found by Kimelman et al. (1979)] and at 328 nm in DOC are indicative of nonpolar tryptophan environments (Longworth, 1971). The inset to Figure 1 shows that the M13-CP tryptophan fluorescence is efficiently quenched by addition of 16-doxylstearic acid to DMPC bilayers. The quenching effect appears to be primarily static (i.e., due to tryptophan residues in immediate contact with 16-DS) as a proportional decrease in the fluorescence lifetime is not observed. The total fluorescence decay in both DOC and DMPC is complex, requiring a sum of three or four exponentials for an adequate fit to the data. A comparison of the parameterization of decays at 20 °C is given in Table I. The values of the reduced χ^2 statistic and other fit quality criteria (weighted residual and residual autocorrelation plots) indicate that a three-exponential sum fits the data adequately in DOC but rather poorly in DMPC, where an extra lifetime must be included to fit the early decay time region. The parameters of the quadruple-exponential analyses and the average lifetimes ($\langle\tau\rangle$) derived from them are very similar in DOC and DMPC. Further interpretation of the decay parameters is of dubious value as the underlying decay law is not necessarily a sum of exponentials even though this functional form can be fitted to the data. This lack of specificity in the fitting function originates from the multiple photophysical and environmental causes of nonexponential tryptophan fluorescence decay in proteins (Creed, 1984; Beechem & Brand, 1985; Engh et al., 1986; Tanaka & Mataga, 1987; Hudson et al., 1987). An alternative parametric comparison can be obtained by using an exponential series fitting function (James & Ware, 1986). Lifetime distributions obtained by this procedure in DOC and DMPC at 20 °C are shown in Figure 2. Although the detailed form of the distributions cannot be physically interpreted, it is clear that they are very similar for the two protein environments. Similar multimodal profiles to those shown in Figure 2 were observed when the same analysis procedure was applied to data collected at other temperatures. The analysis reproduces the overall features of the discrete exponential sum fits (Table I), namely, enhanced short time decay in DMPC resulting in a slightly shorter average lifetime relative to DOC. The approximate lifetimes (mean of τ_i in DOC and DMPC) obtained in the discrete quadruple-exponential analyses are marked on the lifetime axis of Figure 2.

Fluorescence Anisotropy Decay in DOC. A comparison of fluorescence anisotropy decays of M13-CP tryptophan-26 in DOC and DMPC at 20 °C is shown in Figure 3. Analyses of anisotropy decays in DOC as a function of temperature in

Table II: Fluorescence Anisotropy Decay [$r(t)$] Parameters for M13-CP Tryptophan-26 in DOC

T (°C)	r_1[b]	ϕ_1 (ns)	r_2[b]	ϕ_2 (ns)	r_0	χ^2[a]
4.5			0.263	20.54 ± 0.13	0.263	1.149
4.5[c]	0.028	2.31 ± 0.37	0.245	23.83 ± 0.51	0.273	1.017
20.0			0.251	12.46 ± 0.07	0.251	1.294
20.0	0.034	1.57 ± 0.21	0.232	14.26 ± 0.23	0.266	1.116
45.0			0.228	6.76 ± 0.04	0.228	1.509
45.0	0.098	2.52 ± 0.20	0.146	10.91 ± 0.55	0.244	1.205

[a] Includes total fluorescence decay fit with triple-exponential function. [b] ±0.002. [c] Four independent measurements at this temperature gave r_1 = 0.027 ± 0.001 and ϕ_1 = 2.22 ± 0.58 ns (mean ± standard deviation).

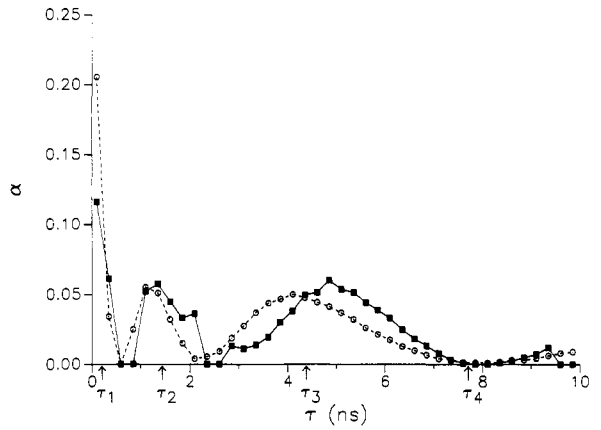

FIGURE 2: Exponential series analysis of tryptophan-26 total fluorescence decays in DOC (■) and DMPC (○) at 20 °C. The lifetime grid is 40 × 0.25 ns starting at 0.1 ns. Reduced χ^2 values for the fits were 0.998 (DOC) and 1.114 (DMPC). Arrows labeled τ_1, τ_2, τ_3, and τ_4 represent the approximate lifetimes obtained in quadruple-exponential analyses (Table I).

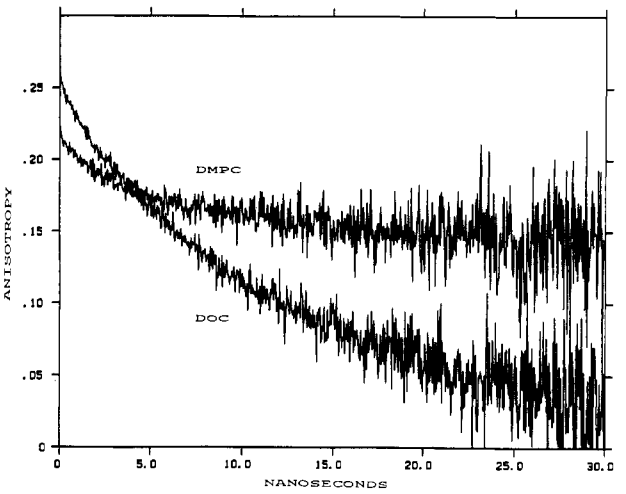

FIGURE 3: Fluorescence anisotropy decays of tryptophan-26 in DOC and DMPC at 20 °C. The curves are constructed directly from the measured polarized decays [$I_V(t)$ and $I_H(t)$ for V polarized excitation] according to $r(t) = [I_V(t) - GI_H(t)]/[I_V(t) + 2GI_H(t)]$. G is the collection efficiency scaling factor $\int I_V(t)/\int I_H(t)$ for excitation perpendicular to both V and H collection planes. This factor (typically 1.05) was determined independently for each experiment with an estimated precision of ±0.01.

terms of single- and double-exponential functions are shown in Table II. It should be noted that the anisotropy decay parameters are essentially independent of the number of lifetimes (3 or 4) used to represent the total fluorescence decay in both DOC and DMPC. The data indicate only small-amplitude subnanosecond reorientational motions of tryptophan-26 as the fundamental anisotropy (r_0) is quite close to the value of 0.3 expected for a completely immobile indole chromophore at the pertinent excitation and emission wavelengths (Valeur & Weber, 1977; Ludescher et al., 1988). The slightly lower values of r_0 observed can be partly ascribed to limited short-time resolution due to truncation of the analysis range (see Materials and Methods). At the lowest of the three temperatures examined (4.5 °C), the resolved anisotropy decay can be well fitted to a single-exponential function representing the rotational rate of the detergent/protein complex. Modeling of this motion in terms of simple hydrodynamics at all three temperatures is shown in Figure 4. The theoretical correlation times (ϕ_p) for a spherical unhydrated particle of molar mass M_m = 17 kg·mol^{-1}, on the basis of a 16:2 mol/mol detergent/protein complex (Makino et al., 1975), are derived from the Stokes–Einstein relationship:

$$\phi_p = M_m \nu \eta / RT$$

where η is the solvent viscosity (taken from the CRC Handbook of Chemistry and Physics, 59th ed.) and $\nu = 0.75 \times 10^{-3}$ m^3·kg^{-1}. The experimental data show a satisfactory linear relationship as prescribed by the model, and the approximate factor of 2 difference between the experimental and theoretical correlation times can be attributed to neglect of hydration in the calculation of the molar volume and to the spherical approximation of particle shape (Cantor & Schimmel, 1980). However, as indicated in Table II, the single-exponential anisotropy decay function results in a successively worse fit

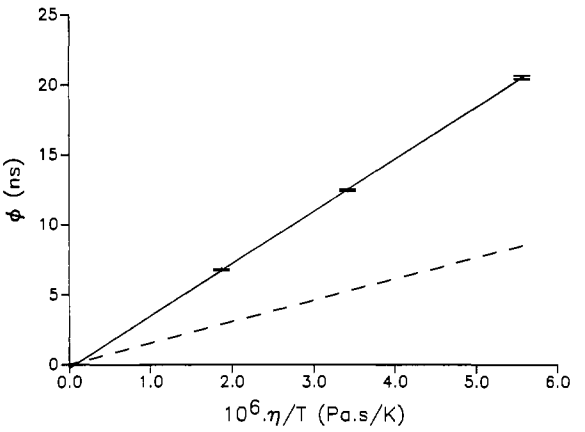

FIGURE 4: Viscosity/temperature dependence of rotational correlation times of M13-CP in DOC from single-exponential anisotropy decay analyses (—) compared to a Stokes–Einstein hydrodynamic model relationship (---). Linear regression fit to experimental data points (horizontal bars bisected by vertical error bars) is extrapolated to zero viscosity.

quality (represented by the reduced χ^2) as the temperature increases. A second rotational component can be resolved with a correlation time of about 2 ns and an angular amplitude which increases with temperature.

In order to address the question of whether this change in the tryptophan rotational dynamics is associated with the environment-dependent conformational equilibrium observed using ^{19}F NMR by Wilson and Dahlquist (1985), a series of anisotropy decay measurements at 4.5 °C (chosen to maximize the population of the MCII conformation; Wilson & Dahl-

Table III: Fluorescence Anisotropy Decay Parameters and Average Lifetimes for M13-CP Tryptophan-26 as a Function of pH in DOC at 4.5 °C

pH	r_1[a]	ϕ_1 (ns)	$\langle\tau\rangle$[b]	χ^2[c]
7.5	0.260	21.33 ± 0.15	5.28	1.152
8.5	0.263	20.54 ± 0.13	5.22	1.149
9.1	0.259	21.07 ± 0.15	5.28	1.170
11.5	0.257	15.53 ± 0.13	2.88	1.299

[a] ±0.001. [b] Defined as in Table I. Units: nanoseconds. [c] Includes total fluorescence decay fit with triple-exponential function except at pH 11.5 (four exponentials).

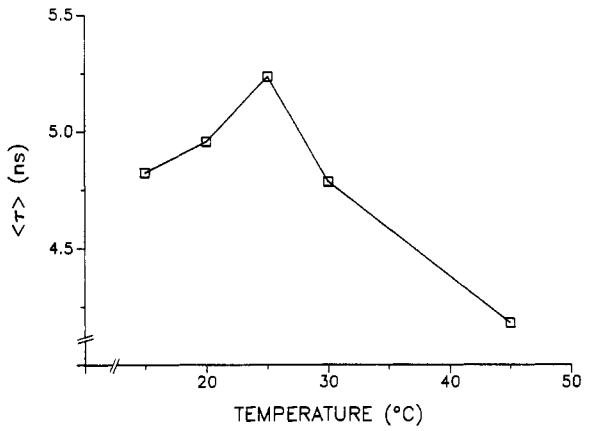

FIGURE 5: Thermal variation of average lifetime ($\langle\tau\rangle$) of M13-CP tryptophan-26 in DMPC bilayers. Values plotted are formulated according to the definition given in Table I from the sum of four exponential fit ($\chi^2 < 1.2$) parameters.

quist, 1985) and variable pH was conducted. Increasing pH has the same effect on the NMR-monitored conformational equilibrium as raising the temperature (Wilson & Dahlquist, 1985). Analysis of the data in terms of single-exponential functions is summarized in Table III, showing no detectable change in the rotational behavior or the average excited-state lifetime in the pH range 7.5–9.1. Analysis of the data in terms of a biexponential anisotropy decay (not shown) leads to the same conclusion. The sharp reduction in the average lifetime recorded at pH 11.5, which is accompanied by a red shift of the fluorescence emission spectrum (approximately 5nm at peak), is probably due to the combined quenching effects of energy transfer to tyrosinate and excited-state deprotonation of the indole imino group (Longworth, 1971). The reduction in the rotational correlation time at pH 11.5 does not reflect rapid motion unresolved in the analysis as the value of r_0 remains similar to that at lower pH.

Fluorescence Anisotropy Decay in DMPC. Total fluorescence intensity decays of M13-CP tryptophan-26 in DMPC bilayers in the temperature range 15–45 °C reveal a maximum in the average lifetime ($\langle\tau\rangle$, defined in Table I) around the lipid phase transition temperature (23 °C) as shown in Figure 5. The complexity of the decay expression required to adequately fit the data did not vary in the temperature range studied. The individual lifetime and amplitude parameters recovered by these analyses are not reported as there is no definitive physical basis at present for interpreting their variation. The fluorescence anisotropy decay of tryptophan-26 in DMPC at 20 °C is shown in Figures 3 and 6. More particularly, Figure 6 illustrates the quality of fit to the measured polarized fluorescence decays for different functional anisotropy decay forms. Two terms are required for an adequate fit, and a second decay term ($r_2\phi_2$) gives a slightly superior fit (Table IV, Figure 6) compared to a constant long time anisotropy [$r(\infty)$] for the inclusion of an additional adjustable parameter. Both the overall anisotropy decay profile and the fit quality differences between the functional forms shown in Figure 6 typify the behavior observed throughout the experimental temperature range (see also Figure 3 and Table IV). Anisotropy decay variation with temperature is

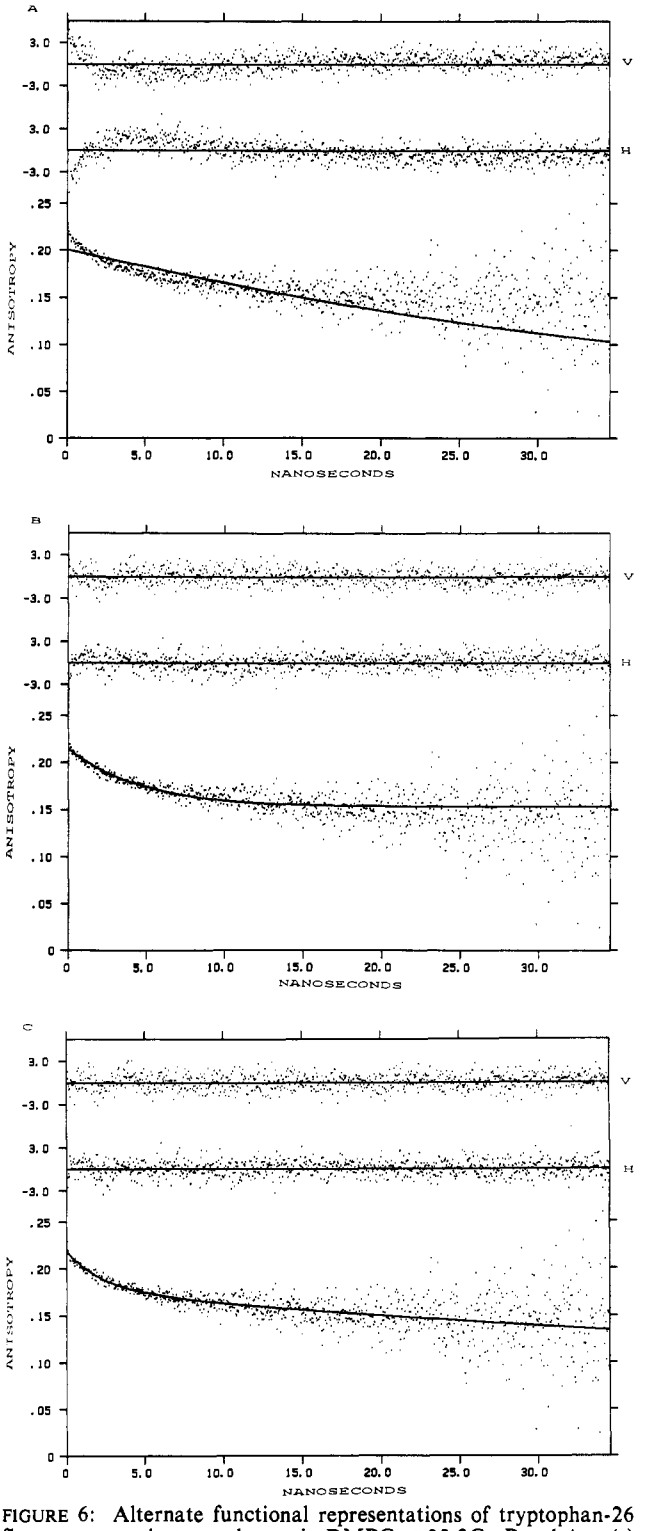

FIGURE 6: Alternate functional representations of tryptophan-26 fluorescence anisotropy decays in DMPC at 20 °C. Panel A: $r(t) = r_1 \exp(-t/\phi_1)$ ($\chi^2 = 1.924$). Panel B: $r(t) = r_1 \exp(-t/\phi_1) + r(\infty)$ ($\chi^2 = 1.163$). Panel C: $r(t) = r_1 \exp(-t/\phi_1) + r_2 \exp(-t/\phi_2)$ ($\chi^2 = 1.110$). In each panel, the upper two plots represent the weighted residuals from the simultaneous fits of the total fluorescence and anisotropy decay functions to the measured vertically (V) and horizontally (H) polarized fluorescence decays. The lower plot shows the analytic anisotropy decay function (solid line) superimposed on (not directly fitted to) the anisotropy decay data (points) formulated as described in Figure 3.

Table IV: Variation of Fluorescence Anisotropy Decay Parameters with Temperature for M13-CP Tryptophan-26 in DMPC Bilayers

	two-exponential decay model						one-exponential + constant model				
T (°C)	r_1[a]	ϕ_1 (ns)	r_2	ϕ_2 (ns)	r_0	χ^2[b]	r_1	ϕ_1 (ns)	$r(\infty)$	r_0	χ^2[b]
15	0.046	2.02 ± 0.14	0.181	163.2 ± 14.2	0.227	1.030	0.058	3.65 ± 0.14	0.164	0.222	1.075
20	0.048	2.23 ± 0.15	0.175	127.3 ± 9.7	0.223	1.110	0.065	4.30 ± 0.15	0.153	0.218	1.163
25	0.049	2.89 ± 0.23	0.181	121.8 ± 10.9	0.230	1.091	0.072	5.42 ± 0.20	0.154	0.226	1.133
30	0.050	1.52 ± 0.08	0.180	66.0 ± 2.2	0.230	1.207	0.080	5.02 ± 0.14	0.138	0.218	1.403
45	0.053	1.96 ± 0.14	0.171	61.6 ± 3.3	0.224	1.219	0.087	4.97 ± 0.17	0.130	0.217	1.306

[a] All angular amplitudes (r) are ±0.001 (±0.002 for r_0). [b] Includes total fluorescence decay fit with four-exponential sum function.

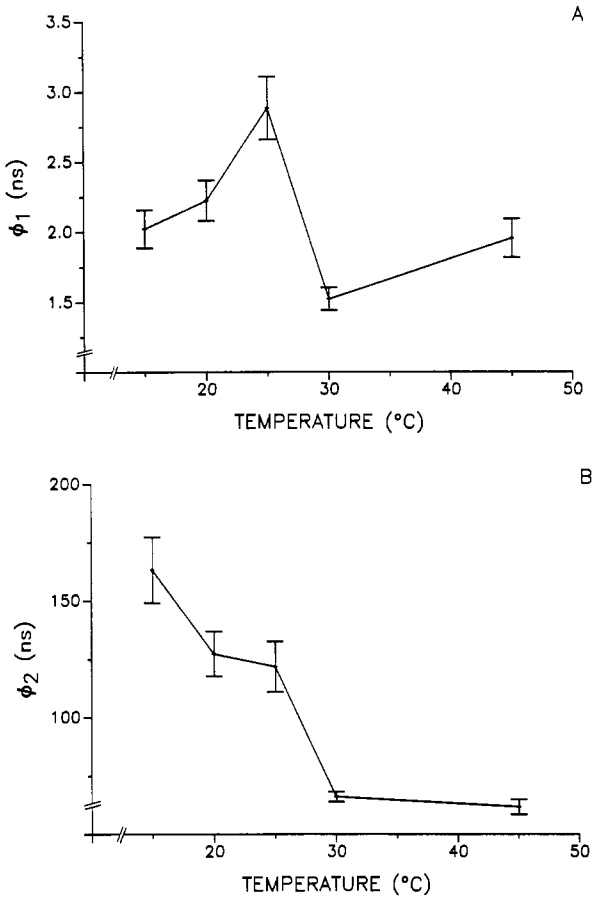

FIGURE 7: Thermal variation of rotational correlation times ϕ_1 (panel A) and ϕ_2 (panel B) from biexponential representation (Table IV) of tryptophan-26 anisotropy decay in DMPC.

summarized in Table IV in terms of both biexponential and single-exponential plus constant parameters. In the biexponential representation, the long correlation time (ϕ_2) shows a marked decrease above the lipid phase transition temperature, as shown in Figure 7B. If a constant second component is used, its value varies as approximately the $r_2\phi_2$ product. Whichever model is used, the short rotational component shows qualitatively the same behavior, with ϕ_1 showing a discontinuous thermal variation across the lipid phase transition (Figure 7A) while the angular amplitude (r_1) shows a continuous increase. These considerations indicate that the two-component resolution is fairly stable. The value of the resolved fundamental anisotropy (r_0) is slightly lower (0.23 cf. 0.25) than that observed in DOC micelles (Figure 3). This decrease is partly attributable to depolarization caused by light scattering in the phospholipid/protein suspensions. Experiments using diluted samples showed that this effect reduced r_0 by about 5% and was time independent.

Discussion

Tryptophan Fluorescence in DOC and DMPC. The fluorescence decay behavior of M13-CP tryptophan-26 in DOC and DMPC is highly complex, requiring a sum of four exponentials or alternatively a multimodal lifetime distribution to adequately fit data with high signal/noise characteristics. It is interesting to assess the possible origins of this decay complexity as the lipid bilayer environment of tryptophan-26 has low aqueous exposure (Hagen et al., 1979; Chamberlain et al., 1978) and most of the nearby amino acid side chains are aliphatic (Asbeck et al., 1969; Nakashima & Konigsberg, 1974). The primary exceptions are tyrosine-24, which is a potential quencher (Tanaka & Mataga, 1987), and methionine-28, which has only weak quenching efficiency in model systems (Johnson & Hudson, 1989). The amide groups of the peptide backbone are also potentially very efficient quenchers (Johnson & Hudson, 1989). Additionally, quaternary interactions including resonance energy transfer between adjacent tryptophan residues must be considered as M13-CP is dimeric in detergent micelles (Makino et al., 1975) and may have the same (Florine & Feigenson, 1987; Bayer & Feigenson, 1985; Nozaki et al., 1976, 1978) or a higher (Datema et al., 1987a,b, 1988a,b) aggregation state in phospholipid bilayers. It is difficult to further refine this list of potential decay complexity sources without a more detailed knowledge of the topology of the M13-CP complex than currently exists (Wickner, 1977; Bayer & Feigenson, 1985). Consequently, only a general interpretation of the total fluorescence decays as a characteristic of a combination of structural and dynamic properties of the tryptophan residue environment is possible. Analysis of our data using two different parametric representations (Table I, Figure 2) shows that the fluorescence decays of M13-CP tryptophan-26 in DOC and DMPC are very similar. There is only a 2% difference between the average excited-state lifetimes in the detergent and phospholipid (Table I). The inference of this result is that the differences between the tryptophan environment of M13-CP in DOC and DMPC at 20 °C are minor. This conclusion is supported by the similarity of the corresponding steady-state fluorescence spectra (Figure 1). Although conformational multiplicity of M13-CP has previously been inferred from CD (Nozaki et al., 1978; Williams & Dunker, 1977; Fodor et al., 1981), Raman (Fodor et al., 1981; Dunker et al., 1982), and NMR (Wilson & Dahlquist, 1985) spectroscopy, the consensus of physical studies of the structure and dynamics of M13-CP to date appears to be that the stable micelle and membrane-associated forms are substantially similar (Nozaki et al., 1976; Chamberlain et al., 1978; Henry et al., 1986, 1987; Leo et al., 1987). Our fluorescence decay data and steady-state spectra appear in accordance with this consensus in respect of the region adjacent to the tryptophan residue. In DMPC, there is a discontinuity in the variation of the average lifetime ($\langle\tau\rangle$, Figure 5) close to the DMPC phase transition temperature of 23 °C, corresponding to similar variations of the steady-state tryptophan fluorescence intensity reported by Wickner (1976) and Kimelman et al. (1979) for samples prepared by the cholate dilution method. This observation indicates that the immediate environment of tryptophan-26 is partially composed of phospholipid acyl chains. This conclusion is substantiated

by the efficient contact quenching of tryptophan fluorescence by the acyl nitroxide 16-DS (Figure 1) as previously observed for nitroxide-labeled phospholipid acyl chains by Florine and Feigenson (1987).

Fluorescence Anisotropy Decay in DOC. Fluorescence anisotropy data indicate only a minor extent of rapid (subnanosecond) reorientational motion for tryptophan-26 in DOC micelles. A simple hydrodynamic model of the rotational diffusion of the detergent/protein complex based on its known composition (16:2 mol/mol; Makino et al., 1975) gives a quite reasonable representation (within the limiting assumptions) of the observed anisotropy decay. However, the data also reveal evidence of more complex reorientational behavior, particularly at higher temperature. The observation of a biexponential anisotropy decay has basically two possible physical origins: rotational diffusion of a rigid ellipsoidal particle (Steiner, 1983) or motion of the protein within the particle independent of the overall rotation. On the basis of the rigid ellipsoid model, the angular amplitudes (r_i) would be expected to be constant unless the particle shape was temperature dependent. Recent electron spin resonance and X-ray scattering studies (Esposito et al., 1987) indicate that pure DOC micelles are ellipsoidal and that the ellipticity is temperature dependent. Of course, the direct relevance of these findings to the M13-CP/DOC complex is questionable. The independent internal motion interpretation requires that the putative overall particle rotational correlation time (ϕ_2) follow a similar hydrodynamic relationship to that shown by the correlation times from the single-exponential fits (Figure 4). Plots of ϕ_2 (Table II) against η/T do not yield a satisfactory linear relationship or zero intercept. The shorter correlation time (ϕ_1) does not show a rational temperature dependence although the uncertainties associated with this parameter make any conclusion rather tenuous. We conclude that the rates of the two rotational processes are poorly resolved at the present data quality level and that the rate and amplitude of the minor component are small enough to allow the application of the single-exponential decay modeled in terms of spherical particle motion without major distortion.

The increased biexponential character of the anisotropy decay in DOC at higher temperatures does not appear to be associated with the pH- and temperature-dependent conformational equilibrium observed by Wilson and Dahlquist (1985). No pH effect in the range 7.5–9.1 at 4.5 °C was observable in the fluorescence anisotropy decay, in contrast to the NMR spectra of ^{19}F-labeled tyrosines-21 and -24 (Wilson & Dahlquist, 1985). It should be emphasized that there is no reason a priori to expect a positive association between the fluorescence and NMR observations. Wilson and Dahlquist (1985) concluded from derived enthalpy considerations that the conformational change detected by their NMR experiments was globally extensive. Although the tryptophan fluorescence anisotropy technique primarily probes structure and dynamics at a local level, propagation of global conformational changes at this level is currently one of the most interesting questions accessible with modern instrumentation. The decrease of the fluorescence lifetime in DOC at pH 11.5 is probably trivial, as discussed above. The accompanying decrease in the rotational correlation time is most simply explained by a decrease in the size of the micelle.

Fluorescence Anisotropy Decay in DMPC. In DMPC vesicles, the absence of overall particle rotation (estimated to be on the order of 10^{-3} s) as a depolarization mechanism in the experimental time regime is demonstrated by the high residual long-time anisotropy. The question then arises of whether the anisotropy reaches a constant value within this time range, as expected for a microscopically oriented system (Szabo, 1984; Kinosita et al., 1984). The present data are somewhat equivocal on this point, primarily due to the signal to noise quality at long time, despite extensive data collection. For completeness, we note the physical implications of both the single-exponential plus constant and biexponential parametric data representations. The value of the constant, $r(\infty)$, reflects the degree of spatial restriction opposing reorientation of the fluorophore (Szabo, 1984; Kinosita et al., 1984). In the present case, the shape of the reorienting potential must clearly be lipid dependent, presumably through direct coupling to acyl chain motion. The more interesting possibility implied by the biexponential analysis is that the tryptophan residue is rigid enough to detect very slow protein motion within the bilayer, represented by the correlation times ϕ_2. The most likely source of a slow protein reorientation with the observed strong rate dependence on the lipid bilayer physical state appears to be axial rotational diffusion (Saffman & Delbrück, 1975; Peters & Cherry, 1982), if it is assumed that the transition dipole of tryptophan-26 is not colinear with the rotation axis. To assess whether a submicrosecond correlation time could result from this reorientational process, an approximate calculation was made of the rotational diffusion constant (D_R) for M13-CP in DMPC at 30 °C according to the expression derived by Saffman and Delbrück (1975) in which the protein is modeled as a cylinder. With the use of input parameters based on the M13-CP dimer volume used in the hydrodynamic calculation for DOC micelles (see above) and a membrane "viscosity" of 1 P (Saffman & Delbrück, 1975), a value of $1/D_R = 1.1$ μs was obtained. This value is at the low end of the range of experimentally measured inverse rotational diffusion constants of membrane proteins (Kinosita et al., 1984) and is consistent [in terms of the Saffman and Delbrück (1975) model] with the lateral diffusion constants of M13-CP in DMPC measured by Smith et al. (1979) using photobleaching techniques. The corresponding fluorescence anisotropy correlation time would be less than $1/D_R$ by an amount dependent on the orientation of the tryptophan transition dipole with respect to the rotation axis (Kinosita et al., 1984). However, fluorescence anisotropy decay due to protein axial rotation should reach an asymptotic limit [$r(\infty)$] which is again dependent on the transition dipole orientation (Kinosita et al., 1984). Inclusion of an additional $r(\infty)$ term in the biexponential anisotropy decay analyses could not be statistically justified [χ^2 remained the same with $r(\infty)$ fixed at several different values]. We conclude that the present data time range requires extension, preferably by tryptophan phosphorescence detection, to fully resolve a correlation time corresponding to protein rotational diffusion from the anisotropic limit $r(\infty)$. The origin of the long correlation times ϕ_2 is of interest since detection of rotational processes of this duration by tryptophan fluorescence anisotropy decay measurements is unusual, but not unprecedented (Beechem & Brand, 1985). We note that axial rotational diffusion of M13-CP in lipid bilayers was not observed in two recent NMR studies (Leo et al., 1987; Datema et al., 1988a), probably as a result of protein aggregation (Datema et al., 1988a) as further discussed below. The rapid restricted motion represented by the rotational correlation time ϕ_1 in both anisotropy decay models is also influenced by lipid dynamics as shown by discontinuous variation across the phase transition (Table IV). Although the values of ϕ_1 obtained (1.5–5.5 ns) primarily represent restricted motion of tryptophan-26, an unresolved component of protein segmental motion may also contribute to this depolarization process.

Summary and Perspective. Irrespective of the functional form used to represent the anisotropy decay, it is clear that the phospholipid environment exerts a marked influence on the reorientational dynamics of tryptophan-26 and also on its fluorescence lifetime. These observations are at variance with results obtained in another time-resolved fluorescence study by Datema et al. (1987a). As the fluorescence intensity and anisotropy decay behavior in detergent micelles (sodium dodecyl sulfate) observed by Datema et al. (1987a) are generally similar to our data in DOC [these two detergents produce substantially similar protein conformational properties (Makino et al., 1975; Nozaki et al., 1978; Henry et al., 1986, 1987)], the origin of the different results obtained in phospholipid bilayers is apparently intrinsic to the lipid/protein preparations. Two potentially significant differences in the M13-CP/phospholipid preparations can be identified: Datema et al. (1987a) used a slightly different lipid composition (20% w/w dimyristoylphosphatidic acid in DMPC) and a different protein incorporation method (detergent dialysis). If the lipid composition were the significant factor, it would imply that there is a preferential interaction of acidic lipids with M13-CP. There is experimental evidence both for (Datema et al., 1987b) and against (Florine & Feigenson, 1987; Kimelman et al., 1979) such interactions. Negatively charged lipids do not apparently affect the bilayer orientation or conformation of fd coat protein (Chamberlain et al., 1978) or M13-CP (Wickner, 1977). A consistent explanation of the results obtained by ourselves and by Datema et al. (1987a) can be formulated on the basis of a difference in the protein aggregation state resulting from the incorporation methods used. Datema et al. (1987a) concluded that the absence of lipid modulation effects on the total fluorescence and anisotropy decays was due to protein aggregation which was also evident from NMR (Datema et al., 1988a,b) and electron spin resonance (Datema et al., 1987b) measurements. Additionally, we note that the decrease of the average tryptophan fluorescence lifetime in phospholipid bilayers relative to detergent reported by Datema et al. (1987a) is considerably larger than the 2% decrease observed in our measurements. Reconstitution methods involving extensive dialysis have been shown to result in some M13-CP incorporation in higher aggregation states than the usual dimer (Nozaki et al., 1978; Dunker et al., 1982; Bayer & Feigenson, 1985). This β-polymer conformation (also known as the "c" conformation; Fodor et al., 1981) is distinguishable from the "50% α" native conformation by its CD spectrum (Fodor et al., 1981; Nozaki et al., 1978). Unfortunately, CD characterization of samples prepared by the cholate dilution technique is precluded by their turbidity (Williams & Dunker, 1977). We interpret our data as demonstrative of a low protein aggregation state on the basis of the following three observations: (1) The fluorescence decay of tryptophan-26 in DMPC is very similar to that in DOC, as is the fluorescence emission spectrum. In DOC, hydrodynamic modeling of the anisotropy decay gives direct evidence of a dimeric aggregation state. (2) The rotational dynamics and fluorescence decay of tryptophan-26 are sensitive to the DMPC thermal phase transition, indicating direct contact with lipid acyl chains. (3) There is efficient quenching of tryptophan fluorescence in DMPC bilayers by 16-DS. The conclusion that M13-CP is in a dispersed low aggregation state with the tryptophan residue in close contact with phospholipid acyl chains is consistent with the results and interpretations of previous studies of this lipid/protein system in this laboratory (Kimelman et al., 1979; Wolber & Hudson, 1982) and elsewhere (Florine & Feigenson, 1987; Bayer & Feigenson, 1985; Nozaki et al., 1976, 1978). On the basis of the interpretation presented above, our results, although different in some respects, are also compatible with those obtained by Datema et al. (1987a).

ACKNOWLEDGMENTS

We thank Suzanne Hudson for providing an excellent library of analysis software and Terry Oas and Lynn Thomason for providing the M13 coat protein samples. Permission to use the SLM fluorometer in the von Hippel laboratory is also gratefully acknowledged.

Registry No. DOC, 83-44-3; DMPC, 18194-24-6.

REFERENCES

Asbeck, V. F., Beyreuther, K., Kohler, H., von Wettstein, G., & Braunizer, G. (1969) *Hoppe-Seyler's Z. Physiol. Chem. 350*, 1047–1056.

Bayer, R., & Feigenson, G. W. (1985) *Biochim. Biophys. Acta 815*, 369–379.

Beechem, J. M., & Brand, L. (1985) *Annu. Rev. Biochem. 54*, 43–71.

Cantor, C. R., & Schimmel, P. R. (1980) *Biophysical Chemistry*, pp 549–570, W. H. Freeman, San Francisco.

Chamberlain, B. K., Nozaki, Y., Tanford, C., & Webster, R. E. (1978) *Biochim. Biophys. Acta 510*, 18–37.

Creed, D. (1984) *Photochem. Photobiol. 39*, 537–562.

Cross, A. J., & Fleming, G. R. (1984) *Biophys. J. 46*, 45–56.

Cross, T. A., & Opella, S. J. (1981) *Biochemistry 20*, 290–297.

Datema, K. P., Visser, A. J. W. G., van Hoek, A., Wolfs, C. J. A. M., Spruijt, R. B., & Hemminga, M. A. (1987a) *Biochemistry 26*, 6145–6152.

Datema, K. P., Wolfs, C. J. A. M., Marsh, D., Watts, A., & Hemminga, M. A. (1987b) *Biochemistry 26*, 7571–7574.

Datema, K. P., van Boxtel, B. J. H., & Hemminga, M. A. (1988a) *J. Magn. Reson. 77*, 372–376.

Datema, K. P., Spruijt, R. B., Wolfs, C. J. A. M., & Hemminga, M. A. (1988b) *Biochim. Biophys. Acta 944*, 507–515.

Dunker, A. K., Fodor, S. P. A., & Williams, R. W. (1982) *Biophys. J. 37*, 201–203.

Engh, R. A., Chen, L. X.-Q., & Fleming, G. R. (1986) *Chem. Phys. Lett. 126*, 365–372.

Esposito, G., Giglio, E., Pavel, N. V., & Zanobi, A. (1987) *J. Phys. Chem. 91*, 356–362.

Florine, K. I., & Feigenson, G. W. (1987) *Biochemistry 26*, 2978–2983.

Fodor, S. P. A., Dunker, A. K., Ng, Y. C., Carsten, D., & Williams, R. W. (1981) in *Bacteriophage Assembly* (Dubow, M. S., Ed.) pp 441–455, Alan R. Liss, New York.

Grinvald, A., & Steinberg, I. Z. (1974) *Anal. Biochem. 59*, 583–598.

Gunst, R. F., & Mason, R. L. (1980) *Regression Analysis and its Applications*, pp 232–234, Marcel Dekker, New York.

Hagen, D. S., Weiner, J. H., & Sykes, B. D. (1979) *Biochemistry 18*, 2007–2012.

Henry, G. D., Weiner, J. H., & Sykes, B. D. (1986) *Biochemistry 25*, 590–598.

Henry, G. D., Weiner, J. H., & Sykes, B. D. (1987) *Biochemistry 26*, 3619–3626.

Hudson, B. S., Ludescher, R. D., Ruggiero, A., Harris, D. L., & Johnson, I. (1987) *Comments Mol. Cell. Biophys. 4*, 171–188.

James, D. R., & Ware, W. R. (1986) *Chem. Phys. Lett. 126*, 7–11.

Johnson, I., & Hudson, B. (1989) *Biophys. J. 55*, 189a.

Johnson, I., Thomason, L., & Hudson, B. (1986) *Biophys. J. 49*, 334a.
Kimelman, D., Tecoma, E. S., Wolber, P. K., Hudson, B. S., Wickner, W. T., & Simoni, R. D. (1979) *Biochemistry 18*, 5874-5880.
Kinosita, K., Kawato, S., & Ikegami, A. (1984) *Adv. Biophys. 17*, 147-203.
Leo, G. C., Colnago, L. A., Valentine, K. G., & Opella, S. J. (1987) *Biochemistry 26*, 854-862.
Longworth, J. W. (1971) in *Excited States of Proteins and Nucleic Acids* (Steiner, R. F., & Weinryb, I., Eds.) pp 319-484, Plenum Press, New York.
Ludescher, R. D., Peting, L., Hudson, S., & Hudson, B. (1987) *Biophys. Chem. 28*, 59-75.
Ludescher, R. D., Johnson, I. D., Volwerk, J. J., de Haas, G. H., Jost, P. C., & Hudson, B. S. (1988) *Biochemistry 27*, 6618-6628.
Makino, S., Woolford, J. L., Tanford, C., & Webster, R. E. (1975) *J. Biol. Chem. 250*, 4327-4332.
Nakashima, Y., & Konigsberg, W. (1974) *J. Mol. Biol. 88*, 598-600.
Nozaki, Y., Chamberlain, B. K., Webster, R. E., & Tanford, C. (1976) *Nature (London) 259*, 335-337.
Nozaki, Y., Reynolds, J. A., & Tanford, C. (1978) *Biochemistry 17*, 1239-1246.
O'Connor, D. V., & Phillips, D. (1984) *Time-correlated Single Photon Counting*, Academic Press, London.
Peters, R., & Cherry, R. J. (1982) *Proc. Natl. Acad. Sci. U.S.A. 79*, 4317-4321.
Ruggiero, A. J., & Hudson, B. S. (1989) *Biophys. J.* (in press).
Saffman, P. G., & Delbrück, M. (1975) *Proc. Natl. Acad. Sci. U.S.A. 72*, 3111-3113.
Smith, L. M., Smith, B. A., & McConnell, H. M. (1979) *Biochemistry 18*, 2256-2259.
Steiner, R. F. (1983) in *Excited States of Biopolymers* (Steiner, R. F., Ed.) pp 117-162, Plenum Press, New York.
Szabo, A. (1984) *J. Chem. Phys. 81*, 150-167.
Tanaka, F., & Mataga, N. (1987) *Biophys. J. 51*, 487-495.
Valeur, B., & Weber, G. (1977) *Photochem. Photobiol. 25*, 441-444.
Wickner, W. (1976) *Proc. Natl. Acad. Sci. U.S.A. 73*, 1159-1163.
Wickner, W. (1977) *Biochemistry 16*, 254-258.
Wickner, W. (1988) *Biochemistry 27*, 1081-1086.
Williams, R. W., & Dunker, A. K. (1977) *J. Biol. Chem. 252*, 6253-6255.
Wilson, M. L., & Dahlquist, F. W. (1985) *Biochemistry 24*, 1920-1928.
Wolber, P. K., & Hudson, B. S. (1982) *Biophys. J. 37*, 253-262.

Application of Fluorescence Photobleaching Recovery To Assess Complex Formation between the Two Envelope Proteins of Sendai Virus in Membranes of Fused Human Erythrocytes†

Ziva Katzir, Orit Gutman, and Yoav I. Henis*
Department of Biochemistry, The George S. Wise Faculty of Life Sciences, Tel Aviv University, Tel Aviv 69978, Israel
Received February 9, 1989; Revised Manuscript Received April 13, 1989

ABSTRACT: Fusion of human erythrocytes by Sendai virions is accompanied by lateral mobilization of the viral envelope proteins (F, the fusion protein, and HN, the hemagglutinin/neuraminidase protein) in the target cell membrane; the dynamic parameters characterizing the lateral diffusion of F and HN in the fused cell membrane are identical [Henis, Y. I., & Gutman, O. (1987) *Biochemistry 26*, 812-819; Aroeti, B., & Henis, Y. I. (1988) *Biochemistry 27*, 5654-5661]. This identity raised the possibility that F and HN diffuse together in the cell membrane in mutual heterocomplexes. In order to investigate the possible formation of F-HN complexes in the target cell membrane, which could be important for the fusion process mediated by the viral envelope proteins, we combined fluorescence photobleaching recovery (FPR) measurements of the lateral mobility of the viral glycoproteins with antibody-mediated cross-linking of F or HN. After fusion, one viral glycoprotein type was immobilized by cross-linking with highly specific bivalent polyclonal IgG. The other glycoprotein type was labeled with fluorescence monovalent Fab' fragments that do not induce cross-linking, and its mobility was measured by FPR. Neither the mobile fraction nor the lateral diffusion coefficient of the Fab'-labeled viral glycoproteins was affected by immobilization of the second viral envelope protein, demonstrating that F and HN diffuse independently in the target cell membrane and are not associated in mutual complexes.

Membrane fusion events are involved in a variety of physiological and pathological processes (Poste & Pasternak, 1978; White et al., 1983; Blumenthal, 1987). The penetration of enveloped viruses into animal cells involves a fusion event, either between the viral envelope and the cellular plasma membrane (as in the case of paramyxoviruses) or between the envelope of lysosomally trapped virions and the lysosomal membrane following adsorptive endocytosis (White et al., 1983). Virally mediated fusion is the best characterized system of biological membrane fusion, and its identification with specific viral envelope proteins (Poste & Pasternak, 1978; Hsu et al., 1979; White et al., 1983; Florkiewicz & Rose, 1984)

† This work was supported in part by Grant 86-00051 from the US-Israel Binational Science Foundation (BSF, Jerusalem, Israel) and by the Fund for Basic Research (administered by the Israel Academy of Sciences and Humanities).
* To whom correspondence should be addressed.

0006-2960/89/0428-6400$01.50/0